

A simple function for mapping induced currents

David Beamish British Geological Survey, Murchison House, West Mains Road, Edinburgh EH9 3LA

Beamish, D., 1987. A simple function for mapping induced currents.
Geophys. J. R. astr. Soc., 90, 485-494.

doi: 10.1111/j.1365-246X.1987.tb00737.x

Summary. A linear inverse method that can be applied to the spatial structure of vertical fields has recently been presented. The application of the method to a regional geomagnetic dataset provided bounds on the lateral and vertical distribution of current concentrations, over a known anomaly. The results obtained by this rigorous analysis are compared with the results that can be obtained using a simple mapping function. The function is the anomalous vertical to anomalous horizontal field-ratio. The high degree of correspondence between the two sets of results confirms that the ratio is a useful, quantitative function for mapping geoelectric boundaries.

Key words: electromagnetic induction, currents, mapping

Introduction

In a recent paper by Banks (1986), a large geomagnetic dataset from northern England was used to investigate the application of a 2-D inverse problem of electromagnetic induction. The inverse problem analysed was that of using the spatial structure of the vertical field, defined along a profile perpendicular to strike, to infer the lateral and vertical distribution of current parallel to strike. Techniques which locate such current concentrations effectively map the structural boundaries of regions of enhanced conductivity. It is generally accepted that vertical fields are much more effective at mapping lateral rather than vertical boundaries (Edwards, Bailey & Garland 1981).

As indicated by Banks (1986), the anomalous magnetic field is a linear functional of the current density from which it derives. If appropriate data exist then the powerful methods which are available for handling linear inverse problems can be applied. The inverse problem is inherently non-unique and realistic constraints, bounding both the magnitude and direction of the induced currents, must be introduced. The problem is not trivial and a detailed account is given by Banks (1986). The dataset used was an 11 -site profile of geo-magnetic field ratios derived from the spatial structure of the vertical and horizontal fields. The southern section of the N-S profile is arrowed and labelled 1 in Fig. 1. The profile was centred on an anomaly at the junction between the Northumberland Trough and Alston Block. Using the field ratios at a period of 750 s, the analysis established that it is very unlikely that a current concentration within the Northumberland Trough alone could account for the observed response. The type of problem analysed inevitably provides a set of acceptable models. A main conclusion of the investigation was that the data appear consistent with a deep basement conductive region whose upper surface lies between 5 and 15 km. The purpose of the present note is to present some previously unpublished results which point out the utility of a simple mapping function which provides results equivalent to those obtained in the thorough analysis conducted by Banks (1986).

The mapping function

The analysis of Banks (1986) and the mapping function considered here, both require inter-site vertical field transfer functions. The mapping function also requires intersite horizontal field transfer functions. The determination of the *separate* quantities for the region was described by Beamish & Banks (1983). Both sets are available at 35 sites with Durham being used as a reference (Fig. 1). The mapping function derived from these data is the anomalous vertical to anomalous horizontal field-ratio $R = Z^a / H^a$. The usefulness of this ratio was emphasized in the forward modelling studies of Summers (1981, 1982).

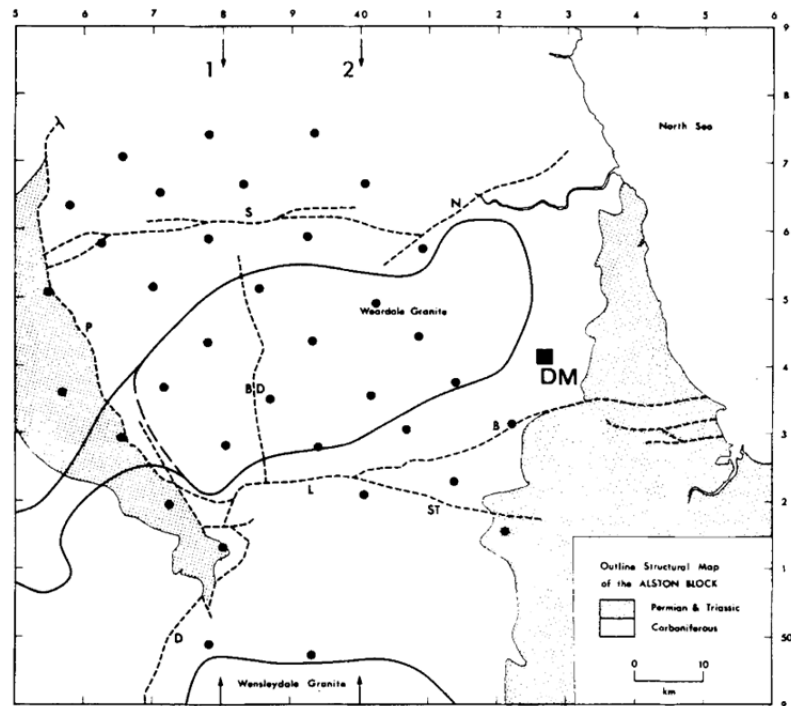


Figure 1 Site locations (solid dots) and simplified geology. Reference site is Durham (DM). Heavy solid line is outline of Weardale granite underlying the Alston Block. Broken lines are regional faults. N-S profiles are arrowed 1 (Banks 1986), and 2 (this study). Coordinate labelling is National Grid, unit 10 km.

The general problem considered by Summers (1981) was the mapping of the equivalent line-current due to a buried and extensive, 2-D conductive region. In essence the results of Summers (1981, 1982) indicated that the ratio R is a simple representation of the gradient of the anomalous field lines where they intersect the surface. Summers designed two high-conductivity anomaly models and carried out numerical investigations. The numerical results obtained have been questioned by Chen & Fung (1986) and Jones (1986a). It seems clear from the detailed reconstructions presented by Chen & Fung (1986) that several implausible results obtained by Summers seem to have arisen from a coding error. The re-analysis undertaken by Chen & Fung (1986) does, however, support Summer's concept of the equivalent line-current based on the anomalous ratio R .

The ratio R has been presented for a number of models by Chen & Fung (1986) and Jones (1986b). In order to illustrate the mapping properties of the ratio, results from a simple 2-D conducting anomaly are now considered. The buried anomaly consists of a rectangular prism 30 km wide in the y -direction and 20 km deep in the z -direction. The horizontal upper surface of the prism is at a depth of 5 km. The resistivity of the prism is 10 ohm.m and it is immersed in an otherwise uniform half-space of resistivity 500 ohm.m. The numerical E-polarization solution for this model was computed using the finite-difference method of Brewitt-Taylor & Weaver (1986). The implementation of the

numerical code has been tested against the recommended 'control' model of Weaver , Le Quang & Fischer (1986) and found to agree to 3 percent on average.

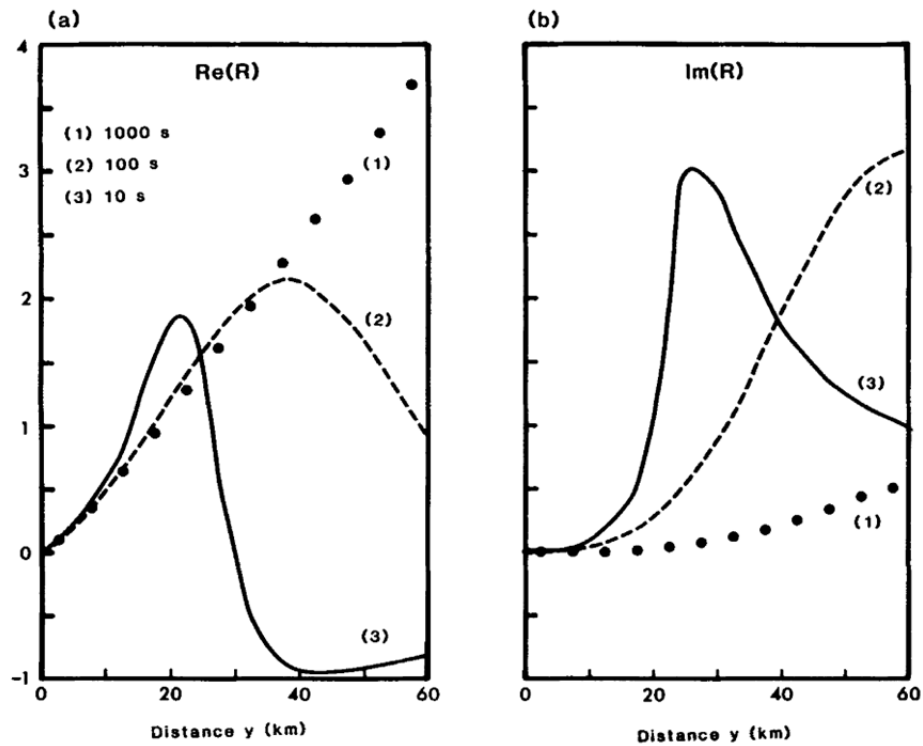


Figure 2 Anomalous field ratio R for the symmetric 2-D model described in the text. One-sided results plotted against distance (y) from the center ($y = 0$) of the rectangular conducting prism, shown in Fig. 3. Results at three periods are shown (1) 1000 s, (2) 100 s, and (3) 10 s. (a) Real part of R . (b) Imaginary part of R .

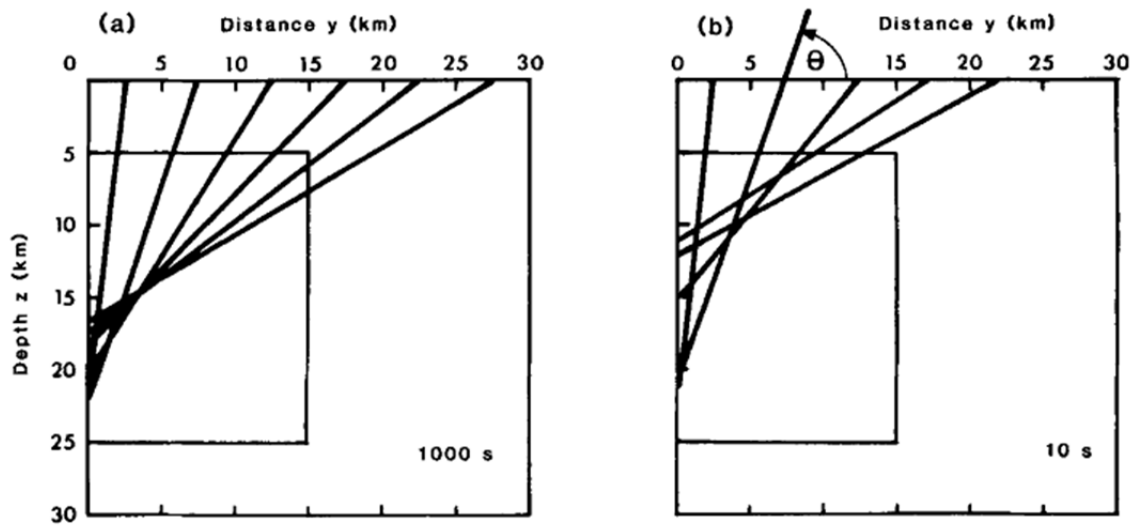


Figure 3 Anomalous field-line radials constructed from the Re (R) model results shown in Fig. 2, for two periods (a) 1000 s and (b) 10 s. The definition of the angle (θ) is given in the text. The inner rectangle shows one-half of the buried conducting region.

Since the anomaly is symmetric, one-sided results are considered about the symmetry axis ($y = 0$ km). The lateral half-width of the conducting region is 15 km. The real (Re) and imaginary (Im) parts of the ratio R are shown in Fig. 2 for three periods (T) of the inducing field. When anomalous vertical fields are considered in relation to single isolated conducting anomalies, the existence of a characteristic period (T_c) is well established (Rokityansky 1982; Chen & Fung 1986). The identification of T_c from field data is an important interpretational aid (Beamish 1985). The same characteristic period is important when considering the behaviour of the ratio R in Fig. 2. For $T > T_c$, then induction is at the inductive limit and frequency-independent behaviour is observed in the ratio R. The limiting behaviour is the quasi-linear spatial gradient observed in Re (R) in the vicinity of the anomalous region. This limiting behaviour is also characterized by a predominantly in-phase response, i.e. $\text{Re}(R) > \text{Im}(R)$. These characteristics can be seen in the $T = 1000$ s curves of Fig. 2. For $T < T_c$, strong spatial variations are observed, except directly above the anomaly where some 'residual' behaviour of the limiting case is observed (e.g. $T = 10$ s, Fig. 2). Intermediate behaviour can be observed in the results obtained for $T = 100$ s. The results of Fig. 2 demonstrate that zero values in both real and imaginary parts of R occur directly above the centre of the conducting region ($y = 0$). The low values of the gradient of Im (R), in the vicinity of the anomalous region, suggest that Re (R) may provide a more reliable mapping function when field data with errors are considered.

The model results are now used to construct anomalous field-line radials as suggested by Summers (1981). Each radial is simply defined by an angle θ between the radial and the surface such that $\cot(\theta) = R = Z^3/H^3$, as a function of position along the profile. The angle θ and the anomalous field-line radials obtained at two of the periods considered above are shown in Fig. 3. Only the real part

of the ratio is considered. The intersection of the radials defines the position of the equivalent anomalous current. The results for $T = 1000$ s (Fig. 3a) can be considered representative of results obtained at the inductive limit. The results obtained for $T = 100$ s (not shown) are almost identical and the 'mapped' position of the anomalous current is independent of frequency. The position is obtained close to, but slightly below, the physical centre of the conducting region. At periods below the inductive limit ($T = 10$ s, Fig. 3b) the position of the equivalent line-current is less precise but extends nearer to the upper surface of the conducting region. These, and other, numerical experiments confirm that for the 2-D case considered, the construction of anomalous field-line radials provides a maximum depth to the upper surface of a conductivity anomaly.

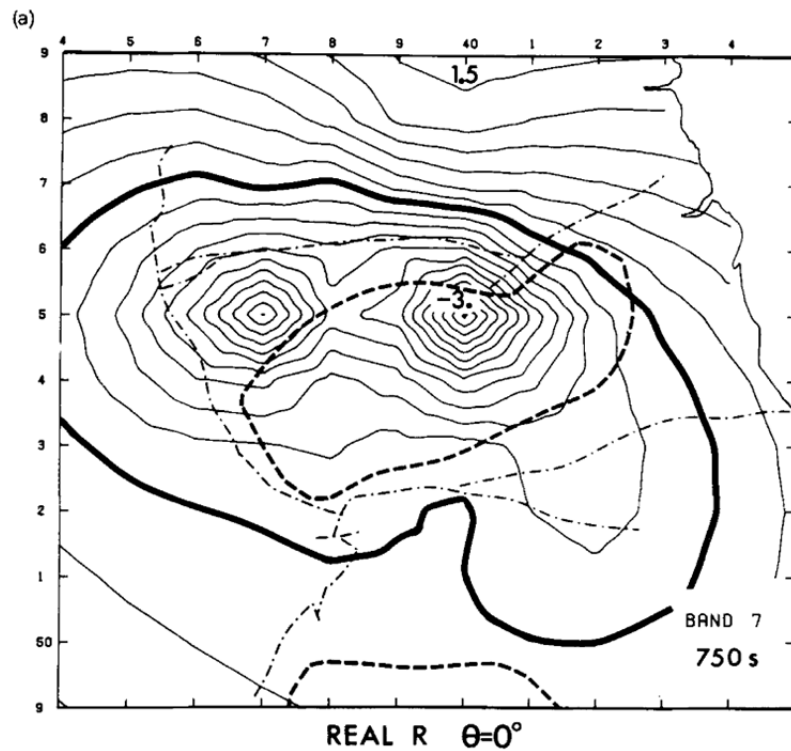


Figure 3 Anomalous field ratio R , for reference field azimuth of zero, period 750 s. (a) Real part. (b) Imaginary part. Contour interval 0.25, zero contours as a heavy line.

The method described above requires no assumptions but accurate inter-site transfer function estimates are needed if stable estimates of the ratio are to be obtained. Since we have a spatial set of the required transfer functions, hypothetical event analysis is used to present maps of the ratio R as a function of the reference horizontal field azimuth. Results are presented for a unit amplitude horizontal field at the reference, polarized in a geographic north direction. This direction was chosen because it corresponds to E-polarization induction in the E-W conductor beneath the

Northumberland Trough (Banks & Beamish 1984). The centre periods of the frequency bands used in the analysis are as follows: Band 1, 5454 s; Band 3, 2727 s; Band 5, 1428 s; Band 7, 750 s; and Band 9, 400 s. As will be demonstrated, the spatial maps for this period interval are associated with the same regional distribution of current flow.

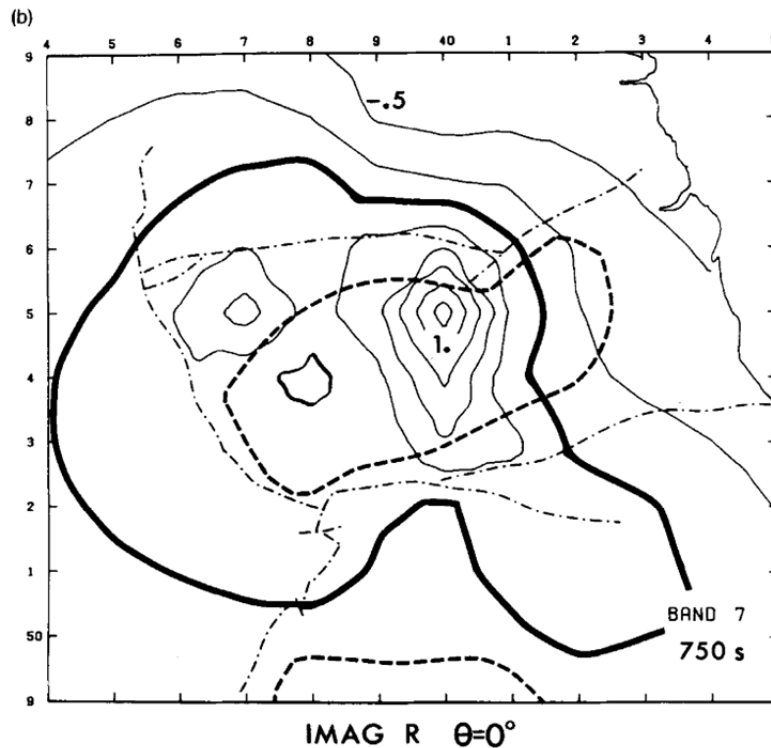


Figure 5 Continued

Lateral mapping

Fig. 4 shows the real part of R at the longest period of the analysis (5454 s) and Fig. 5(a) shows the real part of R at the period (750 s) for which the maximum variation in the ratio is observed. The latter period is the one used in the analysis of Banks (1986). Of particular note is the contour $R = 0$, shown as a heavy line in all the contour plots. This contour effectively maps the lateral position of current 'concentrations', as described in the previous section. Fig. 5(b) shows the imaginary part of R , corresponding to the real part shown in Fig. 5(a). The imaginary part of the ratio increases from a near zero value across the array at the longest period of the analysis to reach a maximum at a period of 750 s as shown in Fig. 5(b). This behaviour is compatible with the model results discussed previously. The model results also indicate that for a valid interpretation, in accord with the forward 2-D model considered, the real and imaginary parts of R should delineate

the same position of $R = 0$, although the gradients will differ. From Fig. 5 we note a good correspondence over a major portion of the $R = 0$ contour. The results across the eastern side of the Alston Block are not well constrained due to a lack of observations.

The variation in position of the $R = 0$ contour, as a function of period, is summarized in Fig. 6. The shaded region defines the bounding locations of the zero contour across the period range from 7200 to 300 s. Again the results in the east are not well constrained but current concentrations are clearly associated with the three main margins of the Alston Block. The main E-W anomaly at the northern margin appears to be highly localized. The feature is elongate and therefore, to a first approximation, 2-D. Vertical and lateral maps of the current concentration associated with this feature are now considered and compared with the results obtained by Banks (1986).

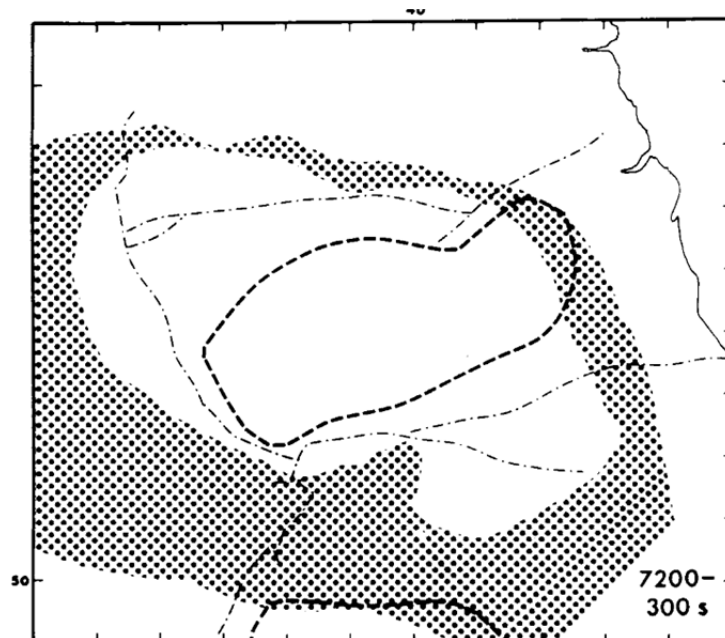


Figure 6 Extent of the spatial variation of the $R = 0$ contour (shaded region), for the period range 7200-300 s.

Vertical and lateral mapping

The maps of the function R , considered above, have been used to provide results along a N-S profile (40 E, arrow labelled 2 in Fig. 1). This profile was chosen since it passes through and bisects the maximum values consistently observed in R , see for example Figs 4 and 5. The values of R have been obtained from the contour values which are necessarily smooth. As an example, the profile observations obtained at a period of 400 s are shown in Fig. 7. Only the 'wavelength' to the south of

$R = 0$ feature is fully defined using the present dataset. The construction of the equivalent field line radials using the profile data is also shown in Fig. 7. The procedure is identical to that previously described. The intersection of the radials defines the position of the equivalent anomalous current. As can be seen in Fig. 7, the result is obtained with a degree of geometrical scatter, both vertically and laterally.

The positions of the equivalent currents obtained as a function of period are shown in Fig. 8. The bandwidth displayed is the same as that considered in the lateral summary map of Fig. 6. Over this bandwidth, the function R appears consistent with a simple 2-D interpretation. Depth estimates of equivalent currents decrease with period from about 20 km (Band 1) to 5 km (Band 7). At shorter periods depths increase as the function becomes unstable. It is worth noting, once again, that the lateral position of the set of equivalent currents is highly constrained and varies by less than 3 km.

The decreasing depth estimates with decreasing period are only consistent with the model results if the shortest periods provide induction well below the inductive limit of the conductive structure. The behaviour of the imaginary part of R , which increases with decreasing period, offers a degree of confirmation that this is the case. From the results shown in Fig. 8 we would estimate the maximum depth to the upper surface of the conductive anomaly as 5 km. The result is obtained at a period of 750 s (Band 7) which displays the largest anomalous field gradients (Fig. 5). The direct equivalence between the simple results obtained in this study and those obtained from the more rigorous appraisal of Banks (1986), indicates the utility of the ratio R as a simple, effective function for mapping induced concentrations of current.

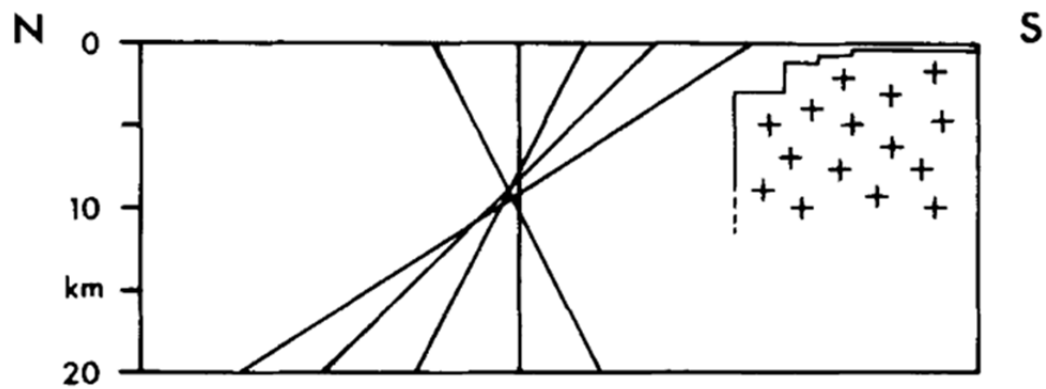
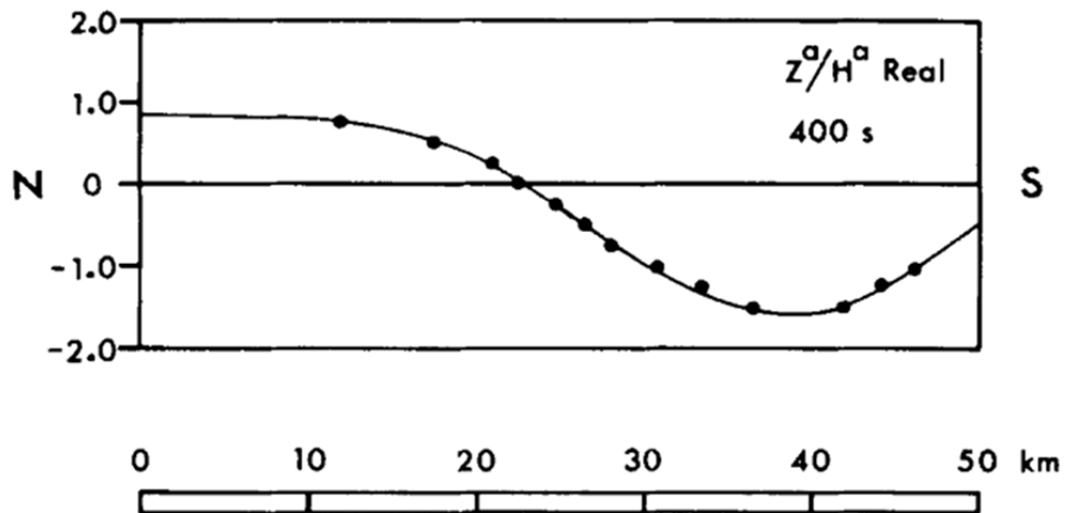


Figure 7 Anomalous field ratio R plotted along a N-S profile at a period of 400 s (upper diagram). Example of construction of anomalous field-line radials (lower diagram).

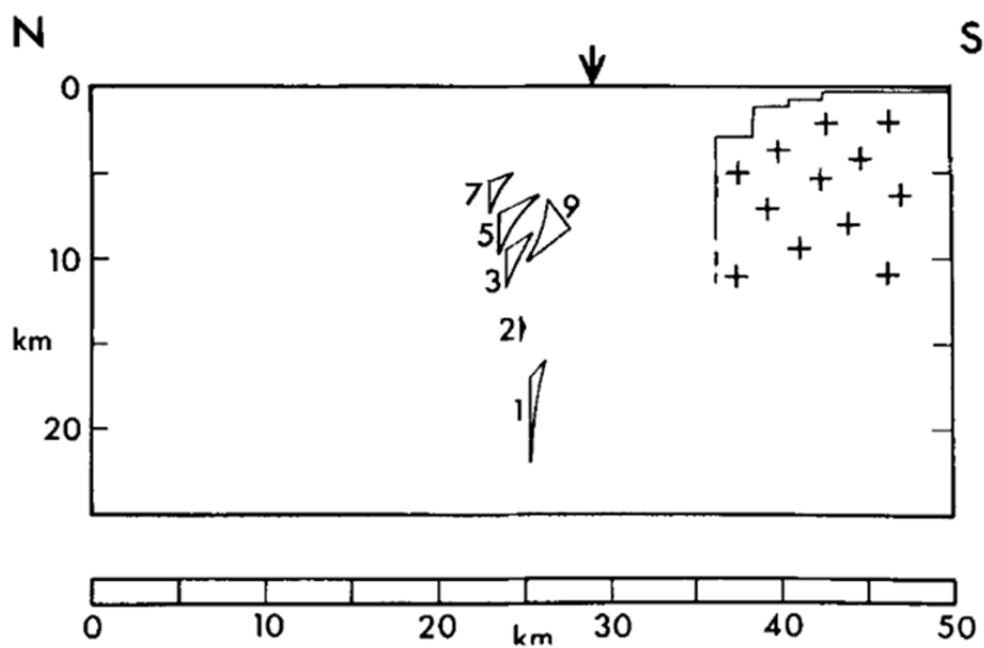


Figure 8 Summary of positions of equivalent currents for the period range 7 200-300 s, along a N-S profile. Period bands labelled 1-9. Weardale granite is outlined in the south. Arrows denote location of the Stublick faults.

Acknowledgments

I am very grateful to Roger Banks for a preprint of the work which prompted this note. I would also like to express appreciation to the two referees and the editor, Peter Weidelt, for their comments on the original version of this note. This paper is published with the approval of the Director, British Geological Survey (NERC).

References

- Banks, R. J., 1986. The interpretation of the Northumberland Trough geomagnetic variation anomaly using two-dimensional current models, *Geophys. J. R. astr. Soc.*, 87, 595-616.
- Banks, R. J. & Beamish, D., 1984. Local and regional induction in the British Isles, *Geophys. J. R. astr. Soc.*, 79, 539-553.
- Beamish, D., 1985. The frequency characteristics of anomalous vertical fields observed in the British Isles, *J. Geophys.*, 57, 207-216.
- Beamish, D. & Banks, R. J., 1983. Geomagnetic variation anomalies in northern England : processing and presentation of data from a non-simultaneous array, *Geophys. J. R. astr. Soc.*, 75, 513-539.
- Brewitt-Taylor, C. R. & Weaver, J. T., 1976. On the finite difference solution of two-dimensional induction problems, *Geophys. J. R. astr. Soc.*, 47, 375-396.
- Chen, P. F. & Fung, P. C. W., 1986. The frequency response of two-dimensional induction anomalies revisited, *J. Geomagn. Geoelectr. Tokyo*, 38, 873-881.
- Edwards, R. N., Bailey, R. C. & Garland, G. D., 1981. Conductivity anomalies: lower crust or asthenosphere? *Phys. Earth planet. Int.*, 25, 263-272.
- Jones, A. G., 1986a. Parkinson's pointers' potential perfidy!, *Geophys. J. R. astr. Soc.*, 87, 1215-1224.
- Jones, A. G., 1986b. On the use of line current analogues in geomagnetic deep sounding, *Geophys.*, 60, 56-62.
- Rokityansky, I. I., 1982. *Geoelectromagnetic Investigation of the Earth's Crust and Mantle*, Springer-Verlag, Berlin.
- Summers, D. M., 1981. Interpreting the magnetic fields associated with two-dimensional induction anomalies, *Geophys. J. R. astr. Soc.*, 65, 535-552.

Summers, D. M., 1982. On the frequency response of induction anomalies, *Geophys. J. R. astr. Soc.*, 70, 487-502.

Weaver, J. T., Le Quang, B. V. & Fischer, G., 1986. A comparison of analytic and numerical results for a two-dimensional control model in electromagnetic induction - II. E-polarization calculations, *Geophys. J. R. astr. Soc.*, 87, 917 -948.